

Disorder-robust p -wave pairing with odd frequency dependence in normal metal-conventional superconductor junctions

Tomas Löthman,¹ Christopher Triola,² Jorge Cayao,^{1,*} and Annica M. Black-Schaffer¹

¹*Department of Physics and Astronomy, Uppsala University, Box 516, S-751 20 Uppsala, Sweden*

²*Los Alamos National Laboratory, Los Alamos, New Mexico 87544, USA*

(Dated: March 16, 2022)

We investigate the induced superconducting pair correlations in junctions between a conventional spin-singlet s -wave superconductor and a disordered normal metal. Decomposing the pair amplitude based on its symmetries in the time domain, we demonstrate that the odd-time, or equivalently odd-frequency, spin-singlet p -wave correlations are both significant in size and entirely robust against random non-magnetic disorder. We find that these odd-frequency correlations can even be generated by disorder. Our results show that anisotropic odd-frequency pairing plays a significant role in disordered superconducting hybrid structures.

Superconductivity arises from the formation and condensation of a macroscopic number of electron pairs, or Cooper pairs. The superconducting state is characterized by the Cooper pair amplitude which, due to the fermionic nature of electrons, is antisymmetric under the exchange of all degrees of freedom describing the paired electron states. These symmetries include the positions, spin, and relative time separation of the two electrons.

In BCS theory of superconductivity the interparticle interaction is instantaneous and, hence, only static, equal-time, pair amplitudes contribute to the order parameter. Such equal-time pair symmetries are then constrained to be either even in space and odd in spin, as in the conventional spin-singlet s -wave state, or odd in space and even in spin (e.g. spin-triplet p -wave). However, even for BCS superconductors, a growing body of evidence suggests that dynamical pair correlations that are odd in the relative time [1–5] can play a role in the physics of superconducting heterostructures [6–8]. Due to their odd time-dependence, these dynamical pair correlations must be either even in space and even in spin or odd in space and odd in spin. Such exotic odd-time pairs are equivalently also referred to as odd-frequency (odd- ω) pairs [1].

A well-established host of odd-time/odd- ω pairs are ferromagnet-superconductor (FS) junctions. In these systems, the combination of spatial invariance breaking due to the interface and spin-singlet to spin-triplet conversion due to the ferromagnet, generates finite odd- ω spin-triplet s -wave pairs in the F region even for conventional spin-singlet s -wave BCS superconductors [9, 10]. The presence of odd- ω s -wave pairs explains several unconventional features of FS junctions, such as the long-range proximity effect [11–19], zero-bias peaks [20, 21], and paramagnetic Meissner effect [22–24].

Odd- ω pairing can also emerge in normal metal-conventional superconductor (NS) junctions. Here the interface allows for both the original even- ω spin-singlet s -wave (isotropic) and an induced odd- ω spin-singlet p -wave (anisotropic) symmetry in the N region [8, 25–27].

However, unlike FS junctions, in NS systems odd- ω pairing has so far been largely ignored. One often-cited reason for this neglect is the argument that p -wave amplitudes are killed in the presence of disorder [28–30]. For example, in the quasiclassical Usadel formulation for disordered systems, only isotropic s -wave solutions are explicitly considered, while any anisotropic part is assumed to be negligible [31]. Additionally, Anderson’s theorem [32] has been invoked to defend the assertion of fragility of p -wave pairs in disordered NS junctions, due to its general notion of fragility of non- s -wave states, even though it does not technically concern proximity-induced effects.

In this work we explicitly show that in NS junctions odd- ω spin-singlet anisotropic p -wave pair correlations are not only robust against disorder but as disorder strength increases, the odd- ω amplitudes constitute a growing fraction of the proximity-induced pair correlations in the N region. Remarkably, we even find odd- ω pairing generated by disorder. We do this by considering a NS junction between a disordered N region and a conventional spin-singlet s -wave superconductor, see Fig. 1, explicitly calculating the fully quantum mechanical time evolution of the proximity-induced superconducting correlations. By showing that odd- ω p -wave pair correlations are ubiquitous and robust, our results provide a completely different view of superconducting pair correlations in disordered heterostructures, with potentially far reaching consequences for the physics, ranging from zero-energy states to paramagnetic Meissner effect.

Model.— To demonstrate the robustness of odd-time/odd- ω pair correlations we study the proximity-induced pair amplitudes in both one-dimensional (1D) and 2D NS junctions between a disordered N region and a conventional spin-singlet s -wave S region, with the interface at $x = 0$, see Fig. 1. The Hamiltonian for these junctions can be written as

$$H = -t \sum_{\langle ij \rangle} c_{i\sigma}^\dagger c_{j\sigma} - \mu \sum_i c_{i\sigma}^\dagger c_{i\sigma} + H_\Delta + H_V, \quad (1)$$

where $c_{j\sigma}$ is the destruction operator for a particle with

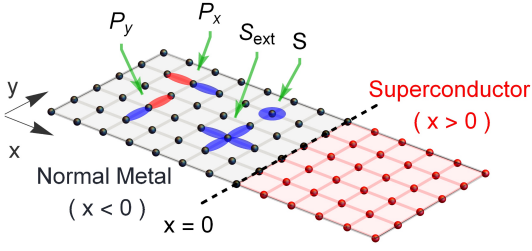


FIG. 1. Sketch of a 2D NS junction with interface at $x = 0$, where filled blue and red circles represent sites in N ($x < 0$) and S ($x > 0$) regions. The relevant spatial orbital symmetries, s -wave, extended s -wave, and $p_{x,y}$ -wave, are depicted in blue (red) for positive (negative) amplitudes.

spin σ at site $j = (j_x, j_y)$ in 2D or $j = j_x$ in 1D, $\langle \dots \rangle$ denotes nearest neighbor sites, t the nearest neighbor hopping amplitude, and μ the chemical potential. The conventional spin-singlet s -wave superconductor is captured by $H_\Delta = \sum_i \theta(x) \Delta c_{i\uparrow}^\dagger c_{i\downarrow}^\dagger + \text{h.c.}$, with Δ being the order parameter and θ the Heaviside step function. We further consider random scalar, or non-magnetic, disorder, so-called Anderson disorder, in the N region through $H_V = \sum_i \theta(-x) V_i c_{i\sigma}^\dagger c_{i\sigma}$, with V_i taken from a uniform distribution on the interval $[-\delta/2, \delta/2]$, where δ is the disorder strength. This type of disorder arises due to non-magnetic impurities or fluctuations in the chemical potential, both inevitable in experimental samples. The length of the N (S) regions are $L_{N(S)}$, measured in units of the lattice spacing $a = 1$.

Pair amplitudes.— The pair amplitudes may be obtained from the time-ordered anomalous Green's function $F_{ij\alpha\beta}(t_2, t_1) = \langle \mathcal{T} c_{i\alpha}(t_2) c_{j\beta}(t_1) \rangle$, where \mathcal{T} is the time-ordering operator. The pair amplitude $F_{ij\alpha\beta}(t_2, t_1)$ accounts for the propagation of quasiparticles from the $(i\alpha)$ -state at time t_1 to the $(j\beta)$ -state at time t_2 . Since $F_{ij\alpha\beta}(t_2, t_1)$ only depends on the relative time difference $\tau = t_2 - t_1$, we focus on the forward time propagation, where the even- (e) and odd-time (o), or equivalently even- and odd- ω , components are extracted as $F_{ij\alpha\beta}^{e(o)}(\tau > 0) = (\langle c_{i\alpha}(\tau) c_{j\beta}(0) \rangle \pm \langle c_{j\beta}(\tau) c_{i\alpha}(0) \rangle) / 2$.

Since no spin-active field is present in NS junctions, pair amplitudes exhibit the same spin symmetry as the parent superconductor. Therefore, we uniquely decompose all pair amplitudes based on their symmetries only in space and time, obtaining

$$d_w^{e(o)}(\tau, R) = \frac{1}{2} \sum_r w(r) \sum_{\alpha\beta} [i\sigma_y]_{\alpha\beta}^\dagger F_{R+r\beta R-r\alpha}^{e(o)}(\tau), \quad (2)$$

with σ_y the y -Pauli matrix, the center of mass $R = (i + j)/2$, and relative $r = (i - j)/2$ spatial coordinates. We study projections of the relative spatial dependence onto the lowest rotation symmetric wave representations: s -wave $w_S(r) = \delta_{|r|=0}$, extended s -wave $w_{S_{\text{ext}}}(r) = (1/z)\delta_{|r|=1}$, and p_i -wave $w_{P_i}(r) = [(\hat{i} \cdot r)/2]\delta_{|r|=1}$, where

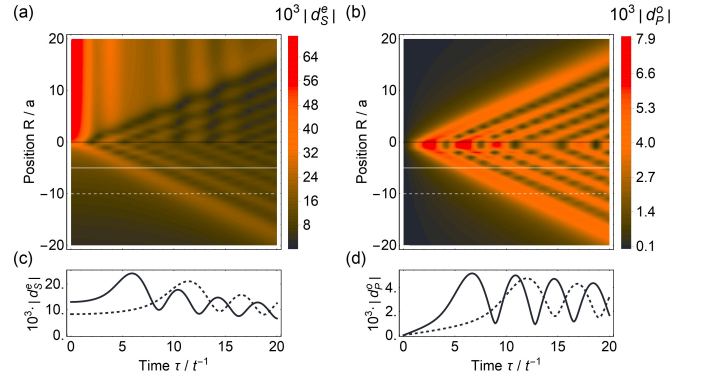


FIG. 2. Even- ω s -wave (a) and odd- ω p -wave (b) pair magnitudes as a function of space and time in clean regime 1D NS junction with interface at $x = 0$. (c,d) Time evolution of the even- and odd- ω pair magnitudes, respectively, with solid (dashed) curve corresponding to the position in N indicated by solid (dashed) lines in (a,b). Parameters: $\mu = 0.25t$, $L_N = 250$, $L_S = 250$, $\Delta = 0.01t$.

z denotes the coordination number.

Evaluation of the pair amplitudes in each symmetry channel in Eq. (2) only requires computation of time-dependent expectation values of the form $\langle c_{i\alpha}(\tau) c_{j\beta}(0) \rangle$. We perform these calculations numerically using the EPOCH (Equilibrium Propagator by Orthogonal polynomial CHain) method for computing the equilibrium propagators, i.e. Green's functions, directly in the time-domain that we have developed in Ref. [33]. In the EPOCH method the equilibrium propagator is expanded in Legendre polynomial mode transients that are recursively computed, allowing us to study both the even- and odd- ω pair amplitudes directly in real space as well as the time domain. As such, this analysis notably goes beyond previous studies of odd- ω pairing [8, 25–27], since the treatment is explicitly in the more natural time domain and also fully quantum mechanical.

Clean regime.— To ultimately understand the pair amplitude behavior in the presence of disorder in NS junctions, we first investigate their time evolution without disorder, $\delta = 0$. In Fig. 2 we show space and time evolution of the magnitude of the even- ω s -wave and odd- ω p -wave pair amplitudes, $|d^{e,o}(\tau, R)|$ in a clean 1D SN junction. We explicitly find no other finite amplitudes with $|r| \leq 1$, apart from even- ω extended s -wave correlations, which shows similar behavior as the s -wave pairing. Notably, the p -wave amplitude is not only non-local and odd in space, but also non-local and odd in the relative time coordinate, fully consistent with previous results studying the time-dependence of odd- ω pair amplitudes [34]. At relative time $\tau = 0$ the even- ω s -wave magnitude of the pair amplitude exhibits a large and constant value in S, due to the finite order parameter Δ in S, as seen in Fig. 2(a). The odd- ω pair magnitude in (b), on the other hand, is necessarily zero at $\tau = 0$. For finite τ both pair

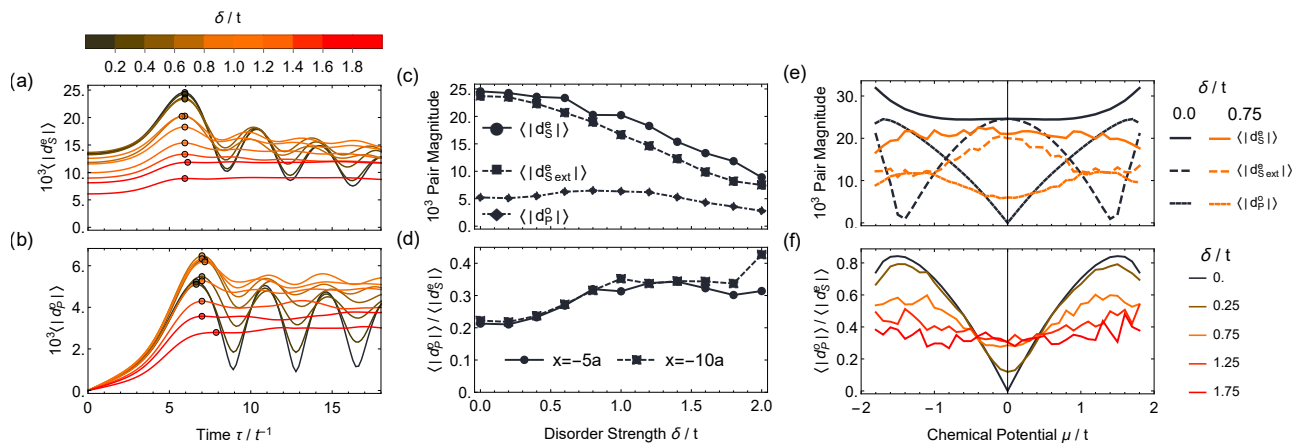


FIG. 3. Even- (a) and odd- ω (b) pair magnitudes at $x = -5a$ in disordered N region in a 1D NS junction, averaged over 60 disorder realizations. Height of the first correlation peak, marked with circles in (a,b), as a function of disorder strength (c) and chemical potential (e) for s -, extended- s -, and p -waves. Ratio between p -wave and s -wave magnitudes as a function of disorder strength (d) and chemical potential (f). Unless otherwise stated, same parameters as in Fig. 2.

amplitudes develop a fan-shaped profile in both S and N regions, albeit with smaller odd- ω magnitudes. The fan profile is due to wave-packed propagation in time and space, with a decay as we move away from the NS interface, since the superconducting proximity effect diminishes with distance [35]. There is also an oscillatory pattern, seen as resonances in Fig. 2(c,d), due to interference between incident and reflected quasiparticle states at the NS interface, as noted before [27, 34, 36, 37]. In particular, the resonance peaks in the N region are a result of the following time evolution process: an electron at x_1 in N has to first propagate towards the NS interface, where it is reflected back as a hole through Andreev reflection, and then propagate back to x_2 in N in order to contribute to the pair amplitude [38]. A simple analytic calculation using a 1D continuum model yields the expected time of this process to $\tau_0 = d/v_F$, where $d = |x_1| + |x_2|$ is the round trip distance and v_F the Fermi velocity, see Supplementary Material (SM) [39] for a complete derivation. This value of τ_0 is fully consistent with the results in Fig. 2(c,d). The overall result is large pair magnitudes that disperse linearly away from the interface in both N and S regions, in agreement with the role of the NS interface as the generator of even- and odd- ω correlations [8, 25–27].

Disorder regime.— Next we turn to the main topic and study the induced correlations in the N region when subjected to scattering by random scalar disorder. In particular, we focus on the behavior of the induced odd- ω p -wave correlations to ascertain whether these induced amplitudes are fragile to disorder as previously assumed [28–30]. In Fig. 3 we present the time evolution of disorder-averaged even- ω s -wave and odd- ω p -wave pair magnitudes for different disorder strengths δ at the fixed position indicated by a solid white line in Fig. 2. At vanishing disorder, we have the situation discussed in Fig. 2, where

both even- and odd- ω pair magnitudes are finite in N but exhibit strong oscillations as they evolve in time. The even- ω correlations, in Fig. 3(a), are insensitive to weak disorder but gradually decay at stronger disorder, while at the same time losing their oscillatory pattern. The odd- ω pair amplitude in Fig. 3(b), on the other hand, actually initially increases in maximum strength for weak disorder, while finally also showing a minor decay with a diminishing oscillatory pattern. The clearly different behaviors of the first resonance peaks, circle markers in Fig. 3(a,b), as disorder increases is evident in Fig. 3(c,d), where we plot the s -wave and p -wave pair magnitudes, as well as their ratio. While both the on-site and extended s -wave correlations monotonically decay with disorder, we find that the p -wave correlations first show a slight increase and then only a very minor decay. Thus, the ratio of odd- ω p -wave to even- ω s -wave correlations *increases* with disorder strength, completely in contrast to naive expectations of disorder fragility for non- s -wave states [28–30]. This conclusion is independent of the specific reference point chosen within the N region. In terms of the oscillatory time-evolution pattern, we find that it persists for small disorder but decays with disorder strength: at $\delta \approx t$, we still find some oscillations, while at very strong disorder, $\delta \approx 2t$ equal to the bandwidth, the oscillations are completely washed out for both even- and odd- ω pair amplitudes.

To examine the stability of these disorder behavior at different parameters, we present in Fig. 3 (e,f) the disorder-averaged pair magnitudes as a function of chemical potential μ , again at the first resonance peak (circles in Fig. 3(a,b)). In the clean regime the even- ω s -wave pair magnitude is almost constant for all values of μ , while the odd- ω p -wave amplitude identically vanishes at half-filling, $\mu = 0$. The latter is due to particle-hole symmetry in the normal state at $\mu = 0$, resulting in a cancellation

of odd-time correlations [40]. While this cancellation of the odd- ω amplitude at $\mu = 0$ in the clean limit occurs in a fine-tuned situation, what is highly relevant for the general understanding of p -wave pairing, is that it still becomes finite at $\mu = 0$ when introducing disorder. Thus disorder can even *generate* p -wave pairing. Furthermore, as seen in Fig. 3(f), where we plot the p -wave to s -wave ratio, p -wave pairing is large, at around 40%, and essentially constant for disorder ranging from moderately weak to very strong. These results highlight the crucial role of non-magnetic disorder, with disorder not suppressing odd- ω p -wave pairing, but even generating it. In terms of other parameter, we have verified that the disorder behavior is not sensitive to the choice of Δ .

The extreme disorder robustness of odd- ω p -wave correlations can be understood, physically, by noting that, in the clean limit, the odd- ω pair correlations induced in an NS junction have their origin in the spatial translation symmetry breaking at the interface. When non-magnetic disorder is added to the N region, this only serves to further disrupt the spatial parity of the electronic states and, therefore, enhance the mixing between the s -wave and p -wave states. Because non-magnetic impurities never mix the spin states, the constraints given by fermion statistics dictate that the p -wave states must have an odd- ω symmetry. In this way, we can understand that odd- ω p -wave pairing should, in general, not only survive non-magnetic disorder but that these pairs should be more robust to disorder than the s -wave pairs. This is in stark contrast to results using quasiclassical theory in the dirty limit where only isotropic s -wave pairing is explicitly considered, while any anisotropic pairing terms are assumed to be very small [31], thus predicting vanishing odd- ω p -wave pairing in NS junction [28–30]. We here also stress that the disorder robustness of odd- ω p -wave correlations is not in contradiction to Anderson’s theorem [32]. Both the s - and p -wave amplitudes in the N region are generated through proximity effect and are consequences of having a bulk s -wave superconductor nearby, with Anderson’s theorem only formally applying to the bulk superconductor.

Beyond 1D.— Above we have only reported results for 1D NS junctions, but higher dimensions show the same results. In the SM we reproduce similar plots to Fig. 2-3 for 2D NS junctions obtained from calculating the time evolution of Eq.(1) for a 2D system. The results are strikingly similar, and also more stable, as they require averaging over fewer disorder realizations to reach converged values compared to the 1D case. This is to be expected as disorder scattering in 2D more quickly evens out any sample differences.

We discover however one striking additional feature in the 2D case. In the clean regime the induced disorder-averaged pair magnitudes in the N region correspond to even- ω s -wave and extended s -wave, and odd- ω p_x -wave symmetries. The absence of p_y symmetry is explained

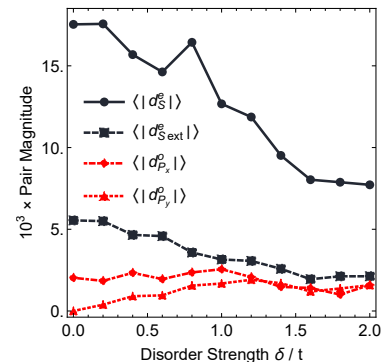


FIG. 4. Disorder-averaged s -wave (black) and p -wave (red) pair magnitudes as a function of disorder strength in a 2D SN junction, taken as the height of the first peak in the time evolution, averaging over 15 disorder realizations. Parameters: $\mu = 0.5t$, $L_{N_{x,y}} = 50$, $L_{S_{x,y}} = 50$, $\Delta = 0.01t$.

by noting that the interface only breaks translation invariance in the x -direction and thus no p_y symmetry can be generated. Still, when we plot all s - and p -wave amplitudes at finite disorder in Fig. 4, we see that the N region hosts both disorder robust and finite odd- ω p_x - and p_y -wave pair amplitudes. The emergence of odd- ω correlations along the y -axis can be understood as a result of translational invariance breaking by the random scatterers also along the y -direction, which allow for a transformation of pair amplitudes into the p_y -wave channel. Notably, Fig. 4 show how both odd- ω p -wave components remain robust with disorder, even initially increasing with increasing disorder strength, whereas the otherwise usually assumed disorder robust isotropic s -wave state instead show a pronounced suppression with increasing disorder. This demonstrates again that p -wave pair amplitudes are highly disorder robust and always constitute a significant portion of induced pairing in NS junctions.

Conclusion.— We demonstrate that odd- ω spin-singlet p -wave pair correlations remain robust against random scalar, or non-magnetic, disorder in NS junctions with a conventional superconductor. In fact, the disorder robustness is higher for p -wave pairing than for the isotropic s -wave components and disorder can even generate odd- ω p -wave pair correlations, even when they are identically zero in the clean regime. As a consequence, odd- ω p -wave correlations always constitute a significant portion of the proximity-induced superconducting pairing also in disordered systems. Our results thus present a completely different conceptual understanding of unconventional odd- ω and p -wave correlations in disordered heterostructures.

We thank A. Balatsky, D. Chakraborty, and T. Löfwander for useful discussions. We acknowledge financial support from the Swedish Research Council (Vetenskapsrådet Grant No. 2018-03488), the European

Research Council (ERC) under the European Unions Horizon 2020 research and innovation programme (ERC-2017-StG-757553), the Knut and Alice Wallenberg Foundation through the Wallenberg Academy Fellows program and the EU-COST Action CA-16218 NanocoHybri.

* Corresponding author: jorge.cayao@physics.uu.se

- [1] V. L. Berezinskii, JETP Lett. **20**, 287 (1974).
- [2] T. R. Kirkpatrick and D. Belitz, Phys. Rev. Lett. **66**, 1533 (1991).
- [3] A. Balatsky and E. Abrahams, Phys. Rev. B **45**, 13125 (1992).
- [4] D. Belitz and T. R. Kirkpatrick, Phys. Rev. B **46**, 8393 (1992).
- [5] E. Abrahams, A. Balatsky, J. R. Schrieffer, and P. B. Allen, Phys. Rev. B **47**, 513 (1993).
- [6] F. S. Bergeret, A. F. Volkov, and K. B. Efetov, Rev. Mod. Phys. **77**, 1321 (2005).
- [7] J. Linder and A. V. Balatsky, Rev. Mod. Phys. **91**, 045005 (2019).
- [8] J. Cayao, C. Triola, and A. M. Black-Schaffer, Eur. Phys. J. Special Topics **229**, 545 (2020).
- [9] F. S. Bergeret, A. F. Volkov, and K. B. Efetov, Phys. Rev. Lett. **86**, 4096 (2001).
- [10] A. Kadigrobov, R. I. Shekhter, and M. Jonson, Europhys. Lett. **54**, 394 (2001).
- [11] V. T. Petrashov, V. N. Antonov, S. V. Maksimov, and R. S. Shalkhal'darov, Pis'ma Zh. Eksp. Teor. Fiz. **59**, 523 (1994).
- [12] M. Giroud, H. Courtois, K. Hasselbach, D. Mailly, and B. Pannetier, Phys. Rev. B **58**, R11872 (1998).
- [13] R. S. Keizer, S. T. B. Goennenwein, T. M. Klapwijk, G. Miao, G. Xiao, and A. Gupta, Nature **439**, 825 (2006).
- [14] T. S. Khaire, M. A. Khasawneh, W. P. Pratt, and N. O. Birge, Phys. Rev. Lett. **104**, 137002 (2010).
- [15] J. Wang, M. Singh, M. Tian, N. Kumar, B. Liu, C. Shi, J. K. Jain, N. Samarth, T. E. Mallouk, and M. H. W. Chan, Nat. Phys. **6**, 389 (2010).
- [16] J. W. A. Robinson, J. D. S. Witt, and M. G. Blamire, Science **329**, 59 (2010).
- [17] M. S. Anwar, F. Czeschka, M. Hesselberth, M. Porcu, and J. Aarts, Phys. Rev. B **82**, 100501 (2010).
- [18] C. Cirillo, S. Voltan, E. A. Ilyina, J. M. Hernández, A. García-Santiago, J. Aarts, and C. Attanasio, New J. Phys. **19**, 023037 (2017).
- [19] Y. Proshin and M. Avdeev, J. Magn. Magn. Mater. **459**, 359 (2018).
- [20] M. Alidoust, K. Halterman, and O. T. Valls, Phys. Rev. B **92**, 014508 (2015).
- [21] A. D. Bernardo, S. Diesch, Y. Gu, J. Linder, G. Divitini, C. Ducati, E. Scheer, M. Blamire, and J. Robinson, Nat. Commun. **6**, 8053 (2015).
- [22] K. Hashimoto, Phys. Rev. B **64**, 132507 (2001).
- [23] F. S. Bergeret, A. F. Volkov, and K. B. Efetov, Phys. Rev. B **64**, 134506 (2001).
- [24] A. Di Bernardo, Z. Salman, X. L. Wang, M. Amado, M. Egilmez, M. G. Flokstra, A. Suter, S. L. Lee, J. H. Zhao, T. Prokscha, E. Morenzoni, M. G. Blamire, J. Linder, and J. W. A. Robinson, Phys. Rev. X **5**, 041021 (2015).
- [25] Y. Tanaka, Y. Tanuma, and A. A. Golubov, Phys. Rev. B **76**, 054522 (2007).
- [26] M. Eschrig, T. Löfwander, T. Champel, J. C. Cuevas, J. Kopu, and G. Schön, J. Low Temp. Phys. **147**, 457 (2007).
- [27] J. Cayao and A. M. Black-Schaffer, Phys. Rev. B **98**, 075425 (2018).
- [28] Y. Tanaka and A. A. Golubov, Phys. Rev. Lett. **98**, 037003 (2007).
- [29] A. A. Golubov, Y. Tanaka, Y. Asano, and Y. Tanuma, J. Phys. Condens. Matter **21**, 164208 (2009).
- [30] Y. Tanaka, M. Sato, and N. Nagaosa, J. Phys. Soc. Jpn. **81**, 011013 (2012).
- [31] K. D. Usadel, Phys. Rev. Lett. **25**, 507 (1970).
- [32] P. Anderson, J. Phys. Chem. Solids **11**, 26 (1959).
- [33] T. Löthman, C. Triola, J. Cayao, and A. M. Black-Schaffer, "Efficient numerical approach to calculate time-dependent green's functions in inhomogenous superconductors," To be published elsewhere.
- [34] C. Triola and A. M. Black-Schaffer, Phys. Rev. B **100**, 144511 (2019).
- [35] T. M. Klapwijk, J. Supercond. **17**, 593 (2004).
- [36] W. L. McMillan, Phys. Rev. **175**, 559 (1968).
- [37] P. Burset, B. Lu, G. Tkachov, Y. Tanaka, E. M. Hankiewicz, and B. Trauzettel, Phys. Rev. B **92**, 205424 (2015).
- [38] Normal reflection is also allowed at the NS interface but can be suppressed in ballistic junctions, and, as shown in Ref. [27], the coexistence of even- and odd- ω correlations can be fully understood in terms of Andreev reflection.
- [39] "See supplemental material at xxxx for additional discussions and figures to support the conclusions,".
- [40] With particle-hole symmetry in the normal state the process of traveling in N towards the junction as an electron and the process traveling away from the interface as a hole identically cancel in the anomalous Green's function, resulting in zero odd-time pair correlations.

Supplemental Material for “Disorder-robust p -wave pairing with odd frequency dependence in normal metal-conventional superconductor junctions”

Tomas Löthman, Christopher Triola, Jorge Cayao,* and Annica M. Black-Schaffer
Department of Physics and Astronomy, Uppsala University, Box 516, S-751 20 Uppsala, Sweden
 (Dated: February 27, 2020)

In this supplementary material we provide details to further support the results and conclusions of the main text.

ANALYTIC TREATMENT OF PAIR AMPLITUDES IN CLEAN NORMAL METAL-SUPERCONDUCTOR JUNCTIONS

In the main text we presented numerical results for the proximity-induced superconducting pair amplitudes in the normal region of normal metal-superconductor (NS) junctions, modeled using a tight-binding Hamiltonian. An important advantage of our numerical approach is that it allows us to easily consider both the clean and disordered regimes, with no approximations. However, since numerical analyses can only be performed for a finite number of parameters, insight can often be gained from a complementary approximate analytic calculation. In this section we study the induced pair amplitudes in a one-dimensional (1D) NS junction in the clean regime analytically using perturbation theory.

Bare Green’s functions

To facilitate our analytic treatment we assume that both sides of the NS junction are infinite and well described by continuum models with dispersions given by $\xi_{\mathbf{k}} = k^2/2m - \mu$ and $E_{\mathbf{k}} = \sqrt{\xi_{\mathbf{k}}^2 + \Delta^2}$, with $\hbar = 1$, for the N and S regions, respectively. Here, m denotes the effective mass of the electrons in both the N and S regions, k is the wave vector, μ is the chemical potential, and Δ is the superconducting order parameter in the S region. Given these dispersions, and first assuming no tunneling between the two regions, it is straightforward to show that the Nambu space Green’s functions in the N and S regions are given by [1, 2]:

$$\begin{aligned}\hat{\mathcal{G}}_S^{(0)}(\mathbf{k}; z) &= \frac{z\hat{\tau}_0 + \left(\frac{k^2}{2m} - \mu\right)\hat{\tau}_3 + \Delta\hat{\tau}_1}{z^2 - \left(\frac{k^2}{2m} - \mu\right)^2 - \Delta^2}, \\ \hat{\mathcal{G}}_N^{(0)}(\mathbf{k}; z) &= \frac{z\hat{\tau}_0 + \left(\frac{k^2}{2m} - \mu\right)\hat{\tau}_3}{z^2 - \left(\frac{k^2}{2m} - \mu\right)^2},\end{aligned}\tag{1}$$

where $\hat{\tau}_i$ ($\hat{\tau}_0$) is the i^{th} Pauli matrix (identity matrix) in the 2×2 particle-hole space and z is a complex frequency allowing us to keep track of Matsubara ($z = i\omega_n$), retarded ($z = \omega + i0^+$), and advanced ($z = \omega - i0^-$) Green’s functions, simultaneously. Note that the pair amplitude, F , is simply given by the off-diagonal matrix element of the Nambu space Green’s function, and, therefore, it is trivially zero in the N region and given by the term proportional to $\hat{\tau}_1$ in the S region in the limit of no tunneling between the two regions.

NS junction

To study proximity-induced pairing in the N region, we assume the NS interface allows local quasiparticle tunneling between the two systems at $x = 0$. In this case, the Dyson equation for the full Nambu-space Green’s function in the N region may be written in real space as:

$$\hat{\mathcal{G}}_N(x_1, x_2; z) = \hat{\mathcal{G}}_N^{(0)}(x_1 - x_2; z) + t_0^2 \hat{\mathcal{G}}_N^{(0)}(x_1; z) \hat{\tau}_3 \hat{\mathcal{G}}_S^{(0)}(0; z) \hat{\tau}_3 \hat{\mathcal{G}}_N(0, x_2; z).\tag{2}$$

This equation can be iterated to obtain a power series expression for $\hat{\mathcal{G}}_N(x_1, x_2; z)$ to arbitrary order in the tunneling, t_0 . Since we are only interested in the qualitative behavior of these expressions we truncate this expansion to leading

order in t_0 :

$$\hat{\mathcal{G}}_N(x_1, x_2; z) \approx \hat{\mathcal{G}}_N^{(0)}(x_1 - x_2; z) + t_0^2 \hat{\mathcal{G}}_N^{(0)}(x_1; z) \hat{\tau}_3 \hat{\mathcal{G}}_S^{(0)}(0; z) \hat{\tau}_3 \hat{\mathcal{G}}_N^{(0)}(x_2; z). \quad (3)$$

The bare Green's functions on the right-hand side of Eq. (3) may be obtained by Fourier transforming the k -space expressions in Eqs. (1) to real space giving:

$$\begin{aligned} \hat{\mathcal{G}}_S^{(0)}(0; z) &= -\frac{im \operatorname{sgn}(\operatorname{Im}\Omega)}{2k_F \Omega} [z g_+^S(z) \hat{\tau}_0 + \Delta g_+^S(z) \hat{\tau}_1 + \Omega g_-^S(z) \hat{\tau}_3], \\ \hat{\mathcal{G}}_N^{(0)}(x; z) &= -\frac{im}{2k_F} [g_+^N(x; z) \hat{\tau}_0 + g_-^N(x; z) \hat{\tau}_3], \end{aligned} \quad (4)$$

where

$$\begin{aligned} g_{\pm}^S(z) &= \frac{1}{\sqrt{1 + \frac{\Omega}{\mu}}} \pm \frac{1}{\sqrt{1 - \frac{\Omega}{\mu}}}, \\ g_{\pm}^N(x; z) &= \frac{e^{i \operatorname{sgn}(\operatorname{Im}z) |x| k_F \sqrt{1 + \frac{z}{\mu}}}}{\sqrt{1 + \frac{z}{\mu}}} \pm \frac{e^{-i \operatorname{sgn}(\operatorname{Im}z) |x| k_F \sqrt{1 - \frac{z}{\mu}}}}{\sqrt{1 - \frac{z}{\mu}}}, \\ \Omega &= \sqrt{z^2 - \Delta^2}, \\ k_F &= \sqrt{2m\mu}. \end{aligned} \quad (5)$$

These expressions can now be inserted into Eq. (3) to find analytic expressions for the Nambu space Green's function in the N region. Note that the bare Green's functions in real space given by Eqs. (4) depend solely on one coordinate as they are the Fourier transform of Eqs. (1) which describe continuum (infinite) systems where translational invariance is not broken.

Proximity-induced pair amplitudes

As we are primarily interested in the induced pair amplitudes in the N region, we focus on the anomalous component of the Green's function in Eq. (3), which is given by:

$$\begin{aligned} F_N(x_1, x_2, ; z) &= -\frac{it_0^2 \Delta \operatorname{sgn}(\operatorname{Im}\Omega) \exp \left[i \operatorname{sgn}(\operatorname{Im}z) \left(|x_1| k_F \sqrt{1 + \frac{z}{\mu}} - |x_2| k_F \sqrt{1 - \frac{z}{\mu}} \right) \right]}{2v_F^3 \Omega} \\ &\quad \times \left(\frac{1}{\sqrt{1 + \frac{\Omega}{\mu}}} + \frac{1}{\sqrt{1 - \frac{\Omega}{\mu}}} \right), \end{aligned} \quad (6)$$

where $v_F = k_F/m$. This expression for the proximity-induced pairing in the N region is exact to order t_0^2 . However, we would like to simplify this expression to gain a better understanding of the physical properties of these pair amplitudes. To proceed, we note that the pair amplitudes are strongly peaked for frequencies $z \sim \Delta$. Moreover, we recall that, in typical superconductors, $\Delta \ll \mu$. Therefore, we assume that $z/\mu, \Delta/\mu \ll 1$ and expand all terms to leading order in these quantities. After a fair amount of algebra we obtain the approximate expression:

$$\begin{aligned} F_N(x_1, x_2, ; z) &\approx -\frac{it_0^2 \Delta}{v_F^3 \Omega} \operatorname{sgn}(\operatorname{Im}\Omega) e^{i \operatorname{sgn}(\operatorname{Im}z) z \frac{|x_1| + |x_2|}{v_F}} \{ \cos [\operatorname{sgn}(\operatorname{Im}z) k_F (|x_1| - |x_2|)] \\ &\quad + i \sin [\operatorname{sgn}(\operatorname{Im}z) k_F (|x_1| - |x_2|)] \}, \end{aligned} \quad (7)$$

which is accurate to leading order in t_0 , z/μ , and Δ/μ .

Proximity-induced pair amplitudes in the time domain

Now when we have relatively compact expression for the proximity-induced pairing in the N region, we wish to make contact with the numerical results in the main text by Fourier-transforming to the time domain. First, we recall

that, in general, a time-ordered propagator is related to the retarded and advanced propagators by:

$$g^T(t) = \int_{-\infty}^{\infty} \frac{d\omega}{2\pi} e^{-i\omega t} [\theta(\omega)g^R(\omega) + \theta(-\omega)g^A(\omega)]. \quad (8)$$

Using this relation, together with the expression in Eq. (7) the time-ordered pair amplitude in the N region may be written as:

$$F_N^T(x_1, x_2; t) = -\frac{it_0^2\Delta}{v_F^3} \int_0^\infty \frac{d\omega}{2\pi} e^{i\omega\tau_0} \left\{ \frac{e^{-i\omega t} e^{ik_F(|x_1|-|x_2|)} + e^{i\omega t} e^{-ik_F(|x_1|-|x_2|)}}{\sqrt{(\omega + i0^+)^2 - \Delta^2}} \right\}, \quad (9)$$

where we define $\tau_0 = \frac{|x_1|+|x_2|}{v_F}$, which corresponds to the total time for a quasiparticle at position x_1 in N to travel towards the NS interface and then back to position x_2 in N, as discussed in the main text. By inspection of the terms within the curly braces in Eq. (9), we see that the proximity-induced pair amplitude possesses both even and odd components in the time variable, t . These even- and odd-time components are given by:

$$\begin{aligned} F^e(x_1, x_2; t) &= -\frac{i2t_0^2\Delta}{v_F^3} \cos[k_F(|x_1| - |x_2|)] \int_0^\infty \frac{d\omega}{2\pi} \frac{e^{i\omega\tau_0} \cos(\omega t)}{\sqrt{(\omega + i0^+)^2 - \Delta^2}}, \\ F^o(x_1, x_2; t) &= -\frac{i2t_0^2\Delta}{v_F^3} \sin[k_F(|x_1| - |x_2|)] \int_0^\infty \frac{d\omega}{2\pi} \frac{e^{i\omega\tau_0} \sin(\omega t)}{\sqrt{(\omega + i0^+)^2 - \Delta^2}}. \end{aligned} \quad (10)$$

Focusing on the odd-time/odd-frequency component, and changing integration variables to $u = \omega/\Delta$, we find:

$$\begin{aligned} F^o(x_1, x_2; t) &= \frac{-t_0^2\Delta}{2\pi v_F^3} \sin[k_F(|x_1| - |x_2|)] \left\{ \int_0^\infty du \frac{e^{iu\Delta(\tau_0+t)} - e^{iu\Delta(\tau_0-t)}}{\sqrt{(u+i\eta)^2 - 1}} \right\} \\ &\approx \frac{-t_0^2\Delta}{2\pi v_F^3} \sin[k_F(|x_1| - |x_2|)] \left\{ -i \int_0^1 du [e^{iu\Delta(\tau_0+t)} - e^{iu\Delta(\tau_0-t)}] \right. \\ &\quad \left. + \int_1^\infty du \frac{e^{iu\Delta(\tau_0+t)} - e^{iu\Delta(\tau_0-t)}}{u} \right\}, \end{aligned} \quad (11)$$

where in the second line we have written the exact integral on the interval $[0, \infty)$ as two approximate integrals: (i) the interval where we assume $\omega/\Delta \leq 1$, and (ii) the interval where we assume $\omega/\Delta \gg 1$. Simplifying these expressions we can write the odd-time/odd-frequency pair amplitude in the N region as:

$$\begin{aligned} F^o(x_1, x_2; t) &= \frac{-t_0^2\Delta}{2\pi v_F^3} \sin[k_F(|x_1| - |x_2|)] \{ E_1[-i\Delta(\tau_0 + t)] - E_1[-i\Delta(\tau_0 - t)] \\ &\quad + 2 \frac{e^{i\Delta\tau_0} [t \cos(t\Delta) - i\tau_0 \sin(t\Delta)] - t}{\Delta(\tau_0^2 - t^2)} \}, \end{aligned} \quad (12)$$

where $E_1(z) = \int_1^\infty e^{-tz}/tdt$ is the exponential integral.

One of the most important features to observe from Eq. (12) is that the last term gives rise to a sharp peak in time, at $t = \tau_0 = \frac{|x_1|+|x_2|}{v_F}$, in full agreement with the numerical results presented in the main text. In fact, this peak has an intuitive origin in the physical processes giving rise to all pair amplitudes in the N region: τ_0 is the amount of time it takes a quasiparticle to complete a trip from x_1 to the interface, reflect as a hole at the interface, and travel back to the point x_2 . Additionally, we note that the expressions given by Eqs. (10) for the even- and odd-time pair amplitudes reveal an oscillatory behavior in both time and space, consistent with the numerical results presented in the main text for the clean regime in 1D. Furthermore, we here see that the periodicity of the spatial oscillations is determined by the Fermi wave vector k_F , while the periodicity of the temporal oscillations is determined by Δ . Lastly, we point out that a similar analysis can be carried out for higher dimensions, where the main features discussed in this part are expected to hold.

Comparison to numerical results in 1D

In Fig. 2(a,b) in the main text we showed that in the clean regime both the even- and odd-time pair amplitudes develop resonance peaks for a finite time separation, which then propagate away from the NS interface, resulting in a

fan-like profile. Here we show that the time separation at which the first resonance peak develops, defining the outer structure of the fan, is the travel time for making the round trip distance to the junction at the Fermi velocity of the normal state.

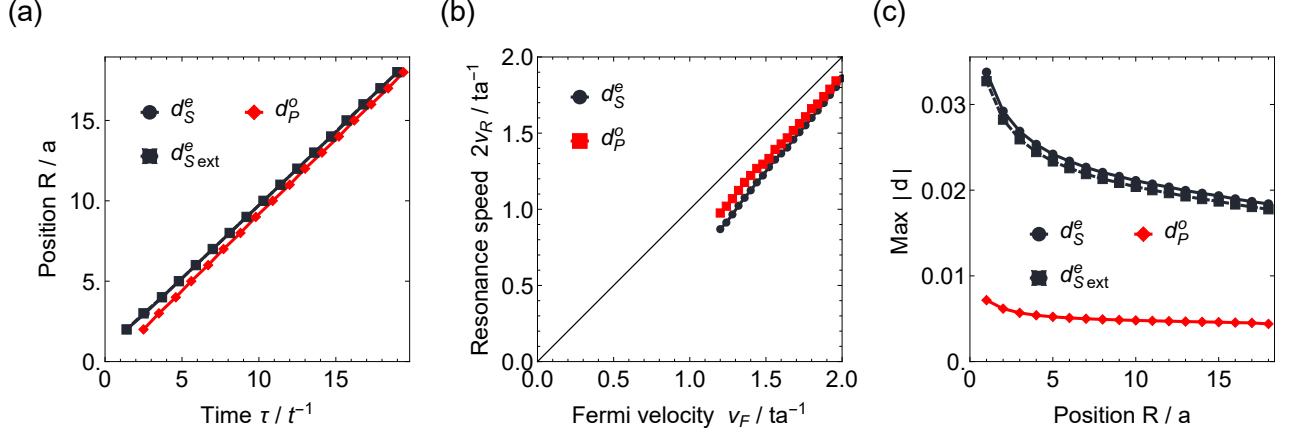


FIG. S1. First resonance peaks of a clean 1D NS junction for the even-time s -wave and extended s -wave (black) and the odd-time p_x -wave (red) pair magnitudes. Parameters are the same as in Fig. 2 in the main text. (a) Resonance peak position as a function of time separation τ . (b) Twice the velocity of the resonance peak $v_R(\mu)$, defined as twice the slope of the line in (a), plotted as a function of the Fermi velocity in N, $v_F(\mu)$, changed by tuning the chemical potential μ . (c) Pair magnitude at the resonance peak as a function of the distance from the NS interface R .

We first show in Fig. S1 (a) that with an increasing time separation, the resonance peaks of Fig. 2 in the main text move linearly away from the junction, implying that the resonance peaks have a definite speed, here called v_R . According to the analytical calculations presented in the previous section, this speed is the Fermi velocity v_F . To test numerically if v_F is indeed the speed in the numerical calculations, it does not suffice to just compute the time separation and position of the resonance peaks as in Fig. S1(a), but rather we need to also manipulate the Fermi velocity v_F , because only then can we observe if the resonance propagation of the resonances is dependent on the Fermi velocity.

The Fermi velocity v_F is defined as the slope of the band dispersion, $v_F = |d\epsilon(k)/dk|$ at the Fermi energy. By changing the chemical potential μ the filling of the band is changed and thus the Fermi energy intersects the energy band $\epsilon(k)$ at new point, with a different slope. Thus, the Fermi velocity v_F is manipulated by the chemical potential μ . If the N region had been infinite, it would have had the band dispersion $\epsilon(k) = 2\cos(k)$ with Fermi velocity $v_F = |d\epsilon(k)/dk| = 2|\sin(k)|$. Even though the N region is finite in the numerical model, we still approach our problem assuming that these ideal expression approximates the band dispersion. With this assumption the Fermi velocity is related to the chemical potential μ through $v_F = \sqrt{4 - \mu^2}$. We can then numerically calculate the speeds of the resonance peaks $v_R(\mu)$ as the slope of the line in Fig. S1(a) by changing μ . Recognizing that R/a on the y -axis in Fig. S1(a) is half the round-trip distance, we in Fig. S1(b) show how the ideal $v_F(\mu)$ relates to $2v_R(\mu)$. We see that the agreement is almost perfectly $v_F(\mu) = 2v_R(\mu)$, exactly as suggested by our analytical results. The minor deviation is easily caused by the fact that changing μ not only changes v_F but also the low-energy density of states and thus the overall size of the pair amplitudes. To conclude, it is the Fermi velocity that sets the speed of the resonance peaks at the NS junction, and the time-separation for the peaks is given by the round-trip distance $2R$. In closing, we also show in Fig. S1(c) that height of the resonance peaks, i.e. the pair magnitude, slowly decays with distance away from the junction for both odd- ω and even- ω due to the inevitable decay of the proximity effect away from the interface.

ADDITIONAL RESULTS FOR 2D NS JUNCTIONS

In the main text we mainly presented the pairing amplitudes for 1D NS junctions. Here we show that the main conclusions that we draw from the 1D system also hold in higher dimensions.

Starting with the clean regime of a 2D junction, we show, in complete analogy with Fig. 2 in the main text, the propagation of even- ω s -wave and the odd- ω p_x -wave pair magnitudes $|d^{e,o}(\tau, R)|$ in Fig. S1. As for the 1D case, the pair magnitudes are obtained from Eq. (2) in the main text. As seen, most aspects of the propagation remains unchanged between 1D and 2D junctions. At equal times $\tau = 0$, the even- ω magnitudes in Fig. S2(a) have a largely

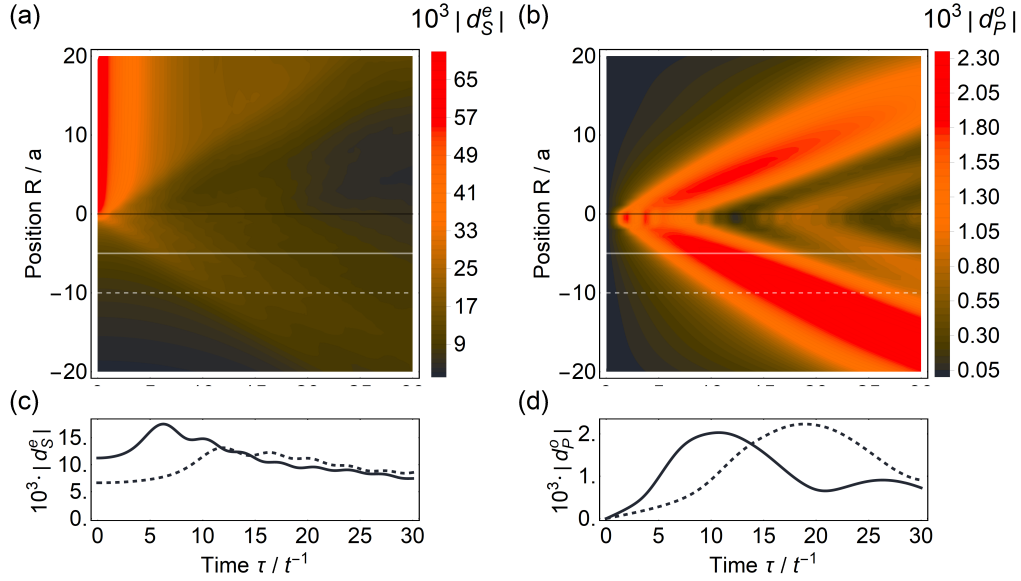


FIG. S2. Even- ω s -wave (a) and odd- ω p_x -wave (b) pair magnitudes in the N region as a function of position from the NS interface R and time τ for a clean 2D SN interface located at $R = 0$. (c,d) Time evolution of the even- and odd- ω pair magnitudes, respectively, with solid (dashed) curve corresponding to the fixed position in N indicated by solid (dashed) lines in (a,b). Parameters: $\mu = 0.5t$ and $\Delta = 0.01t$ on a square NS junction with side lengths $L_S = L_N = 100a$.

constant amplitude inside the S region, which spreads into the N region by proximity effect. In contrast, the odd- ω magnitude at $\tau = 0$ is identically zero by symmetry. At finite time separations $\tau > 0$, we find a ridge of large pair magnitudes, a resonance, linearly emanating away from the NS interface, also in agreement with the 1D results. Thus the broad features remain unchanged between 1D and 2D, although there are also some differences. Most notable from Fig. S2 is the absence of the fan-like oscillatory pattern seen in 1D, and, in addition, the pair resonances are much broader, as clearly seen in the position cuts presented in Fig. S2(c,d). Both of these qualitative differences can be directly interpreted as resulting from the change in dimension. To understand this we return to the physical picture suggested by the pair amplitude time evolution: a quasiparticle making a round-trip from the position R in the N region to the NS interface and then back to R . In the 1D junction, there is only one trajectory for this trip. However, in 2D there are a plethora trajectories besides the shortest path, which is the straight line joining the R point and the point on the NS interface closest to it. These 2D trajectories includes loops and braids that take full advantage of the extra dimension. However, the total length of these trajectories are always longer than the shortest path and thus their associated travel times will be longer. Still, among the likely paths, most will arrive shortly after the round-trip time for the shortest path. As a consequence, similarly as in the 1D junction, the first resonance peak reflects the travel time of the shortest path. The added variations in travel times in 2D however does two things; first, it considerably broadens the first resonance peak; second, it washes out the sharp fan-like oscillatory pattern seen in 1D. This explains all qualitative differences seen in Fig. S2 compared to the 1D junction. As this picture suggests, we also see in Fig. S2 that the width of the first resonance peak widens with R , reflecting that longer paths have more opportunities to deviate. Less evident from Fig. S2, but still worth mentioning, is that in 2D the height of the pair amplitude at the resonance peaks decay faster than in 1D, partly reflecting that peak is broadened, but also that the pair amplitude wave disperse geometrically in 2D unlike in 1D.

Finally we also compare the disordered regimes for 1D and 2D NS junctions. In Fig. S3 we show how the disorder-averaged pair magnitudes $|\langle d_{s(p)}^{e(o)} \rangle|$ evolve with disorder strength δ , similarly as in Fig. 3 in the main text. The main difference is that we in Fig. S3 show all wave projections, including the even- ω s -wave (a) and extended s -wave (b) states, as well as the odd- ω p_x -wave (c) and also the odd- ω p_y -wave (d) states. We see in agreement with the 1D results in the main text that the even- ω waves are monotonically decreasing (apart from statistical fluctuation) with increasing disorder, while the odd- ω p_x -wave instead shows an initial increase. Additionally, we find that the odd- ω p_y -wave, which by symmetry is identically zero in the clean region, is quickly generated by disorder. Thus, considering the relative abundance of odd- ω p -waves to the even- ω s -wave pair magnitudes in Fig. S3(e), we see that the ratio of odd- to even- ω pairing rapidly increases with disorder, with the p_y ratio quickly approaching that of the original odd- ω p_x -wave wave.

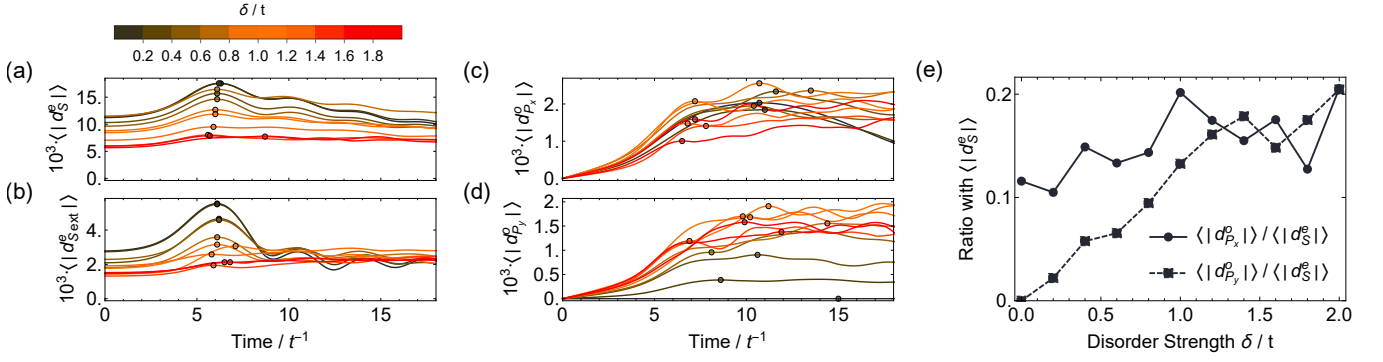


FIG. S3. (a-d) Disorder-averaged pair magnitudes $|\langle d_{s(p_i)}^{e(o)} \rangle|$ at $x = -5a$ in the disordered N region of a 2D NS junction for 15 disorder realizations. (e) The ratio of the first resonance peaks marked by circles in (a-d) for the odd- ω p_x - and p_y -wave magnitudes to the even- ω s -wave magnitude. Unless otherwise stated, same parameters as in Fig. 2.

* Corresponding author: jorge.cayao@physics.uu.se

- [1] A. A. Abrikosov, L. P. Gorkov, and I. E. Dzyaloshinski, *Methods of quantum field theory in statistical physics* (Courier Corporation, 2012).
- [2] G. D. Mahan, *Many-particle physics* (Springer Science & Business Media, 2013).